Korean J. Chem. Eng., 37(11), 2068-2074 (2020)
DOI: 10.1007/s11814-020-0619-x

pISSN: 0256-1115
eISSN: 1975-7220

Effects of carbonization conditions on the microporous structure and high-pressure methane adsorption behavior of glucose-derived graphene

Faten Ermala Che Othman*, Sadaki Samitsu, Norhaniza Yusof*,†, and Ahmad Fauzi Ismail***

*Advanced Membrane Technology Research Centre (AMTEC), School of Chemical and Energy Engineering (SCEE), Universiti Teknologi Malaysia (UTM), 81310 Skudai, Johor Darul Ta'zim, Malaysia
**Data-driven Polymer Design Group, Research and Services Division of Materials Data and Integrated System (MaDIS), National Institute for Materials Science (NIMS), Sengen 1-2-1 Tsukuba, Ibaraki 305-0047, Japan
(*Received 22 March 2020 • Revised 21 April 2020 • Accepted 30 June 2020*)

Abstract−A simple, promising, environmentally friendly, and high yield technique to synthesize high specific surface area (SSA) and porous graphene-like materials from glucose precursor through carbonization and controlled chemical iron chloride ($FeCl_3$) activation was demonstrated. Designing this nanoporous graphene-based adsorbent with high SSA, abundant micropore volume, tunable pore size distribution, and high adsorption capacity, is crucial in order to deal with the demands of large-scale reversible natural gas storage applications. Raman spectroscopy, BET method of analysis, and N_2 adsorption/desorption measurements at −196 °C were adopted to evaluate the structural and textural properties of the resultant glucose derived-graphene (gluGr) samples. The effects of different carbonization conditions, such as the inert environments (argon, helium, and argon) and temperatures (700, 800, 900, and 1,000 °C), have been studied. A glucose-derived graphene carbonized under nitrogen environment at 700 °C (NGr700) with highly interconnected network of micropores and mesopores and large SSA (767 m^2/g) exhibited excellent methane (CH_4) storage property with exceptionally high adsorption capacity, superior to other glucose-derived graphene (gluGr) samples. A maximum volumetric capacity up to 42.08 cm^3/g was obtained from CH_4 adsorption isotherm at 25 °C and 35 bar. Note that the adsorption performance of the CH_4 is highly associated with the SSA and microporosity of the gluGr samples, especially NGr700 that was successfully synthesized by $FeCl_3$ activation under N_2 environment.

Keywords: Glucose-derived Graphene, Graphene-like Materials, Carbonization, Microporous Adsorbent, Methane Adsorption

INTRODUCTION

Since Geim et al. reported on the production of high quality two-dimensional (2D)-monocrystalline graphitic films in 2004 [1,2], graphene materials have attracted tremendous attention. This is due to their unique and extraordinary properties, including large specific surface area (SSA), high intrinsic mobility, high Young's modulus and thermal conductivity, and optical transmittance and good electrical conductivity [3,4]. Various fabrication methods of graphene have been developed, which include chemical vapor deposition, mechanical chemical exfoliation, chemical synthesis, and pyrolysis [5]. Raw materials, fabrication methods, and their processing conditions are three important factors in industry-directed application researches of graphene-like materials, because they predominantly determine molecular structure and materials properties of graphene obtained as well as its production rate and cost. In particular, in spite of numbers of previous studies, the design of the microporous structure of graphene has not been established yet [6]. Therefore, low-cost fabrication of high-quality microporous graphene is still challenging. Among various fabrication methods of graphene, pyrolysis of graphene in "bottom-up" process is promising because of its simple and scalable process. The selection of suitable raw material and appropriate processing conditions is important for optimizing microporous structure of graphene.

There are two categories of low-cost raw materials of graphene mass available from natural resources. One includes agricultural wastes such as rice husks, sugarcane bagasse, corn straw core, almond shells, olive stones [7]. The other covers agricultural raw materials such as biodiesel, milk, palm oil, butter, sugar, and sunflower oil [8]. In general, agricultural wastes are comprised of large amount of silica component [9], whereas agricultural raw materials contain hydrocarbons abundant of glucose units. When synthesizing a precursor for pyrolysis, chemical synthesis is effectively utilized to obtain microporous graphene owing to effects on the pore development and surface characteristics. Precursors obtained by chemical synthesis treatment are further subjected to pyrolysis under inert conditions at high temperature (700-1,000 °C), leading to graphene having various microporous structure depending on chemical features of raw materials and chemical reduction treatment conditions. Various common chemical reagents have been reported as an activating agent depending on chemical features of raw materials, which include potassium hydroxide (KOH) [10], phosphoric acid (H_3PO_4) [11], sodium hydroxide (NaOH) [12], sulfuric acid (H_2SO_4) [13], calcium chloride ($CaCl_3$) [14], iron chloride ($FeCl_3$) [15], zinc chloride ($ZnCl_2$) [16], and magnesium chloride ($MgCl_2$) [17]. For example, alkaline hydroxide, such as potassium hydroxide (KOH) and sodium hydroxide (NaOH), is suitable for activation of agricultural wastes due to the etching effects of KOH on the sil-

†To whom correspondence should be addressed.
E-mail: norhaniza@petroleum.utm.my

ica structure. These activating agents increase micropore width and lead to production of highly porous structures. Pyrolysis using agricultural wastes produces graphene with high thermal stability with nanosized crystalline structure due to the function of silica [18]. In contrast, $ZnCl_2$ and $FeCl_3$ are usually used as chemical activating agents for agricultural raw materials mainly comprised of glucose units. These agents can affect the formation of large surface area and introduce surface functional groups, which develops high surface area, small mesoporosity, high conductivity, and uniform morphology [19,20]. Because of simple chemical structure, glucose is considered as a representative raw material for synthesis of graphene-based adsorbents. Therefore, this study focused on glucose as a raw material for producing graphene-like materials with high surface area. Zhang et al. [21] successfully fabricated high-quality graphene from glucose by utilizing $FeCl_3$ as it acted as both the template and catalyst for the formation of graphene. However, detailed discussion on microporous characteristics of glucose-derived graphene has not been obtained and properly discussed in any previous studies.

In addition to raw materials and fabrication methods, carbonization temperature and environment are also important parameters inn optimizing the microporous structure of graphene suitable for targeted applications. Since most previous studies mainly focused on nanoelectronics, capacitors, batteries, and catalysis [19], the microporous characteristics and applications in gas adsorption and storage have not been fully investigated yet. This current study is aimed at enlightening on the fabrication of microporous glucose-derived graphene (gluGr) using $FeCl_3$ activation, for gas adsorption application. Due to that, the requirement of microporous structures such as high surface area, large micropore volume, and tunable pore size distribution depending on particular gas molecules size was the main focus of this study. In addition, the effects of carbonization condition including type of gases and carbonization study were thoroughly studied in determining the optimized condition for fabrication of gluGr for CH_4 adsorption.

EXPERIMENTAL

1. Synthesis of glucose-derived Graphene (gluGr)

Glucose (≥99.5%; Sigma-Aldrich), iron chloride (anhydrous 98% $FeCl_3$; Alfa Aesar), and concentrated hydrochloric acid (HCl 36%; Merck) were procured from suppliers. At ratio 2 : 1, both glucose and $FeCl_3$ were mixed and dissolved in deionized (DI) water in a porcelain boat to obtain a yellowish mixture with a ratio of 1 : 2 (mixture of glucose and $FeCl_3$: water). The mixture was further heated in an oven for 24 hours under air environment at 80 °C to obtain a caramelized solid mixture. Then, the solid mixture was subjected to carbonization treatment in tube furnace at different carbonization temperature (700, 800, 900, and 1,000 °C) with constant heating rate of 5 °C/min for all samples [21]. Furthermore, the effects of different gas environment such as argon (Ar), helium (He), and nitrogen (N_2) with flow rate of 200 mL/min were studied. After each treatment, the furnace was left for cooling to room temperature under the specific gas flow. The obtained black solid was placed in a beaker with 2 M of hydrochloric acid (HCl) and left for stirring for at least 2 hours. This step is an important step to remove the iron in the graphene sample. After that, the solid sample was washed with DI water for several times until the pH was neutral and the washing was finished with acetone. The sample was sonicated and filtrated by using vacuum filtration. Finally, the sample were left to dry in a vacuum oven at 80 °C for overnight to obtain the final material. The glucose derived-graphene samples were denoted as gluGr throughout this study, meanwhile the gluGr with specific treatment was denoted as AGr, HGr, and NGr for treatment under Ar, He, and N_2, respectively, as shown in Table 1.

Table 1. Glucose-derived graphene (gluGr) samples under different carbonization inert conditions and temperatures.

Sample	Gas	Temperature (°C)
AGr700	Ar	700
HGr700	He	700
NGr700	N_2	700
NGr800	N_2	800
NGr900	N_2	900
NGr1000	N_2	1,000

2. Characterization

The textural characteristics of the resultant gluGr were determined by measuring the N_2 adsorption/desorption isotherms at −196 °C in a Belsorp-max surface area and porosity analyzer (MicrotracBEL Corp., Japan). Prior to the N_2 adsorption measurements, all graphene samples were outgassed under vacuum at 350 °C for at least 1 hour. The data obtained from N_2 adsorption can be utilized in determining the specific surface area by exploiting the Brunauer, Emmett, and Teller (BET) model in the relative pressure (P/P_0) range between 0.05 to 0.20. Meanwhile, the total pore volume was evaluated from the amount of the N_2 adsorbed at P/P_0=0.99 and the micropore volume was estimated by the *t*-plot method. The pore size distribution (PSD) of the graphene samples was obtained by a non-local density functional theory (NLDFT) method. Identification and characterization of chemical and physical properties of the gluGr samples was determined by Raman spectroscopy analysis. This analysis was performed using RAMANplus from Nanophoton equipped with a triple monochromator system to eliminate contribution from the Rayleigh line. All samples were analyzed with a 532 nm argon excitation laser with a power of 1.0 mW at laser exit to avoid thermal effects.

3. Methane Adsorption Measurements

The adsorption equilibrium of CH_4 of the resultant gluGr was measured by volumetric method using a BELSORP-HP adsorption apparatus (MicrotracBEL Corp., Japan). The adsorption isotherms were recorded at 25 °C and up to 35 bar. In this method, the temperature of the adsorption is controlled by using a thermostatic bath utilizing water as the coolant that connected to a circulating jacket in a Dewar bottle. Approximately 0.3 g of the graphene samples was used for the adsorption studies. Prior the adsorption test, the samples were degassed at 350 °C under vacuum environment, in which the temperature was gradually increased from 25, 50, 150, and 350 °C. This is very crucial step prior adsorption test to ensure the elimination of any moisture and organics in the samples. In this study, the final adsorption amount at the terminal

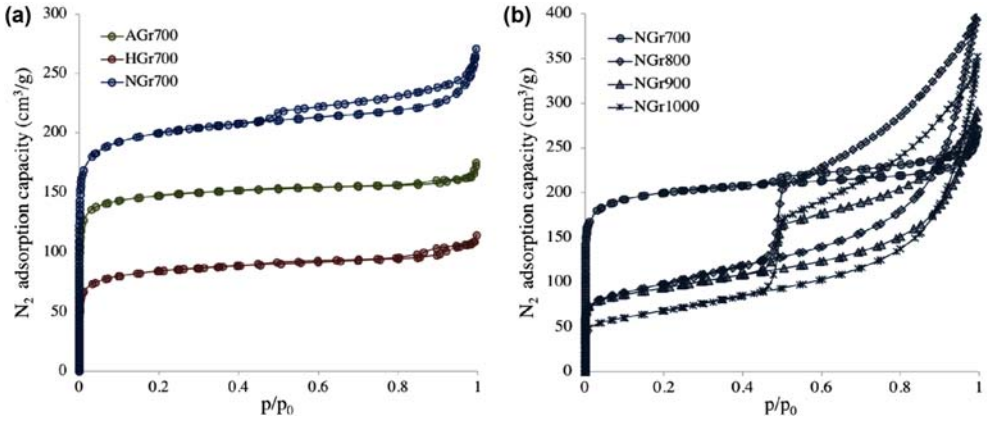

Fig. 1. Nitrogen (N_2) adsorption/desorption isotherms of graphene derived-glucose at −196 °C and different carbonization conditions (a) under different inert gases and (b) under N_2 at different carbonization temperatures.

temperature and pressure is considered as the adsorption equilibrium amount. Ultrahigh purity (99.9%) grade CH_4 gas was used throughout the study.

RESULTS AND DISCUSSION

To investigate the microporosity of the gluGr samples, N_2 adsorption/desorption isotherms of gluGr are presented in Fig. 1. N_2 uptake rapidly increases at low relative pressure region ($P/P_0<0.1$) in all samples, of which behavior corresponds to a Type I adsorption isotherm according to the International Union of Pure and Applied Chemistry (IUPAC) classification [22]. The isotherm curves directly indicate microporous structure of gluGr samples. Depending on carbonization atmosphere (N_2, Ar, and He) at 700 °C the NGr displayed the highest N_2 uptake at the $P/P_0=0.1$, suggesting favorable atmosphere for making large micropore volume. When changing carbonization temperatures (700, 800, 900, and 1,000 °C) under N_2 atmosphere, the N_2 uptake at the $P/P_0=0.1$ evidently decreases with increasing carbonization temperature, suggesting the reduction of micropore volume. Simultaneously to the reduction, the isotherms presented large hysteresis at the P/P_0 of 0.5 to 1.0, indicating the development of mesoporous structure.

By quantitatively analyzing the isotherms using micro- and mesoporous analysis models, the porous characteristics of gluGr samples are summarized in Table 2. When pyrolysis proceeded at 700 °C, NGr exhibited largest SSA as compared with AGr and HGr (Fig. 2(a)). The SSA of the NGr is 146% and 32% higher than that of HGr and AGr. NGr700 also exhibits the highest V_{micro} as compared with AGr and HGr (Fig. 2(c)). The close correlation between V_{micro} and SSA suggests the increase in V_{micro} leading to increase in SSA. In the pyrolysis process, inert condition is generally preferable to obtain microporosity because it effectively removes volatiles gases without preventing undesired burn off and chemical damage of samples [23]. Indeed, Song et al. [24] addressed that carbonaceous materials subjected to pyrolysis under inert gases exhibit more open porous structure and higher gas flux in comparison to those pyrolyzed in vacuum or air.

In addition to carbonization atmosphere, carbonization temperature is probably another important parameter in fabricating

Table 2. Porous characteristics of gluGr samples.

Condition	AGr	HGr	NGr			
Temp. (°C)	700	700	700	800	900	1,000
SSA (m^2/g)	576.3	315.7	761.0	347.4	340.7	238.3
V_{total} (cm^3/g)	0.247	0.131	0.344	0.410	0.246	0.295
V_{micro} (cm^3/g)	0.243	0.160	0.328	0.378	0.240	0.221

microporous structure as it is involved with the thermal energy required to partially break chemical bonds of precursors [24]. Therefore, gluGr samples were synthesized under N_2 atmosphere by varying carbonization temperature between 700-1,000 °C. Interestingly, carbonization temperature significantly affects the microporous structure of gluGr samples. The largest SSA and V_{micro} was obtained at 700 °C, which is 2.2-3.2 times larger than that obtained at 800-1,000 °C (Fig. 2(b)). The SSA decreased remarkably between 700-800 °C, while V_{micro} reduced moderately. At carbonization temperatures between 800-1,000 °C, the gluGr samples resulted in almost the same values of SSA and V_{micro}. At low carbonization temperature, volatile compounds were mildly released from the matrix and formed uniform pore structure with high porosity that contributed to high SSA. On the other hand, at high temperature, the explosive gas evolution leads to formation of irregular pore structure such as cracks and pinholes, which can block and reduce the porous structure. Moreover, higher carbonization temperature may destroy the porous structure of the gluGr, resulting in lower SSA. Another hypothesis is that graphene-like materials often suffer from the restacking between neighboring layers due to strong van der Waals attraction [25], resulting in serious reduction of the accessible surface area, which is partly supported with the Raman results discussed later. The optimum carbonization condition of gluGr is determined as the pyrolysis under N_2 atmosphere at 700 °C.

Fig. 3(a) shows the pore size distribution (PSD) of the gluGr carbonized under different inert conditions (Ar, He, and N_2), while Fig. 3(b) shows the PSD of the samples at two different carbonization temperatures: 700 and 1,000 °C. The PSD was obtained by applying the NLDFT plot to the N_2 adsorption data. There are

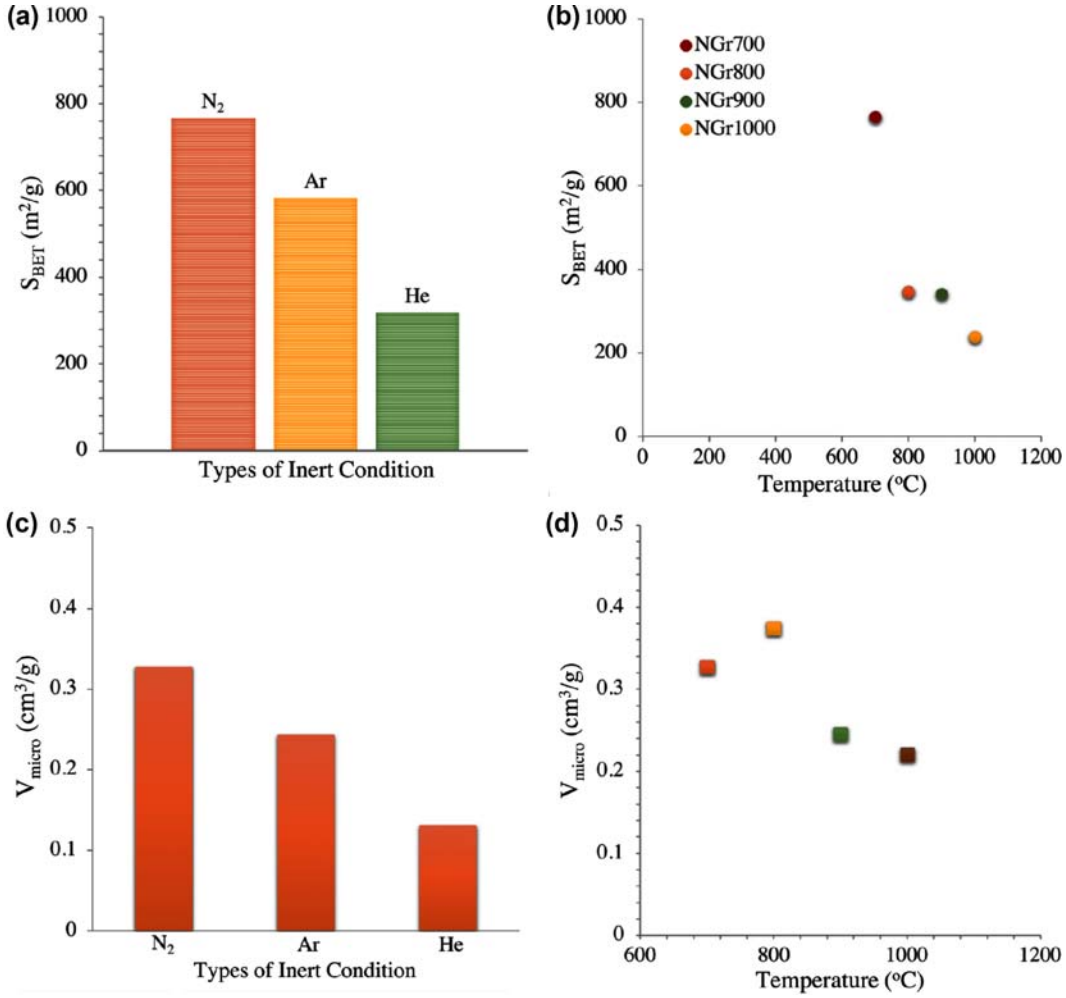

Fig. 2. Porous properties of the resultant gluGr under different carbonization environment and temperatures ((a) and (c)) S_{BET} and V_{micro} of gluGr carbonized under different inert gases and ((b) and (d)) S_{BET} and V_{micro} of gluGr carbonized under N_2 at different temperatures.

no significant differences between the PSD of all samples. The pore size of all resultant samples lies in the micropore range, which is below 2 nm. In Fig. 3(a), two significant peaks can be detected in all samples, ranging between 0.8-1.5 nm, proving the microporosity of the samples. Amongst the samples, NGr700 displays the most intensified, sharpest, and narrowest peak as compared to AGr700, HGr700, and other temperatures. It can be seen that the micropore volume of NGr700 is twice the micropore value of HGr700 and very minimum value of mesopores. This statement is supported by the N_2 adsorption/desorption isotherms above.

It becomes apparent that all resultant carbonized gluGr samples featured well-defined supermicropores extensively interconnected with narrow mesopores, with no apparent macroporosity. It also believed that this hierarchical pore structure is extremely advantageous for high volume CH_4 adsorption applications, since the mesopores will provide a low-resistant pathway for the diffusion of CH_4 molecules, while the micropores will offer more adsorption sites trapping CH_4 [26]. Also, the connectivity of the pores can decrease the diffusion distance and accelerate the migration of CH_4 molecules into the porous system, ensuring fast kinetic uptake [27].

The internal structural characterization of the gluGr was evaluated using Raman spectroscopy in the region 800-3,000 cm^{-1}. Theoretically, in Raman spectra analysis of carbonaceous or graphitic materials, the appearance of two main peaks at 1,350 cm^{-1} and 1,580 cm^{-1} is very crucial that represents the D-band and G-band, respectively [18]. The D-band corresponds to sp^3 C-C bond, which is related to the amorphous, defect, and disordered structures of the graphene samples, while the G-band corresponds to sp^2 C-C bonds, which is related to the order graphite crystalline structure. However, in graphene-like materials, there is an additional band observed in the spectrum at 2,700 cm^{-1} known as 2D-band [28]. This 2D-band originates from phonon scattering process and it is interrelated with the band structure of graphene layers [29]. Accordingly, this 2D-band is the proof of successful synthesizing of gluGr as graphene-like materials.

As can be seen in Fig. 4(a), the Raman spectra of the gluGr samples that was carbonized under N_2 gas flow exhibit the highest intensity, followed by HGr and AGr. Meanwhile, under the N_2 conditions, the other gluGr were carbonized under different temperatures from 700 until 1,000 °C. As can be seen in Fig. 4(b),

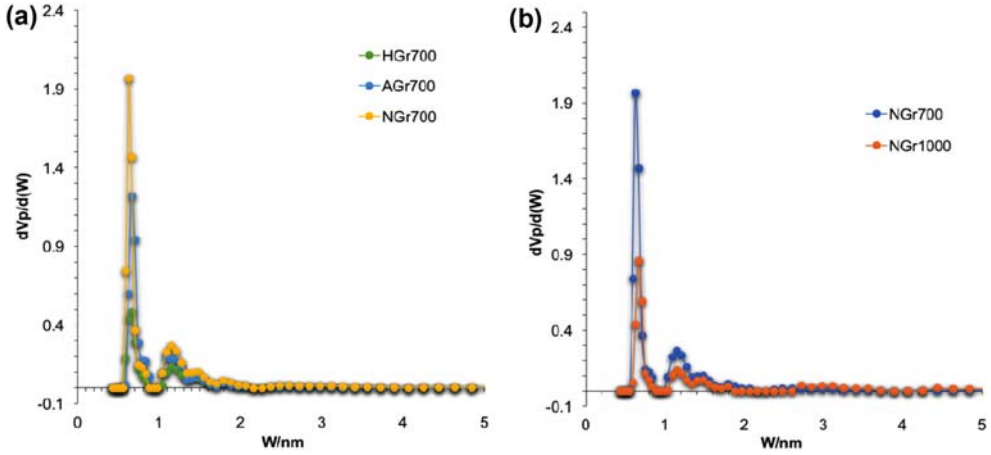

Fig. 3. Pore size distribution of gluGr under different (a) inert conditions; and (b) temperatures.

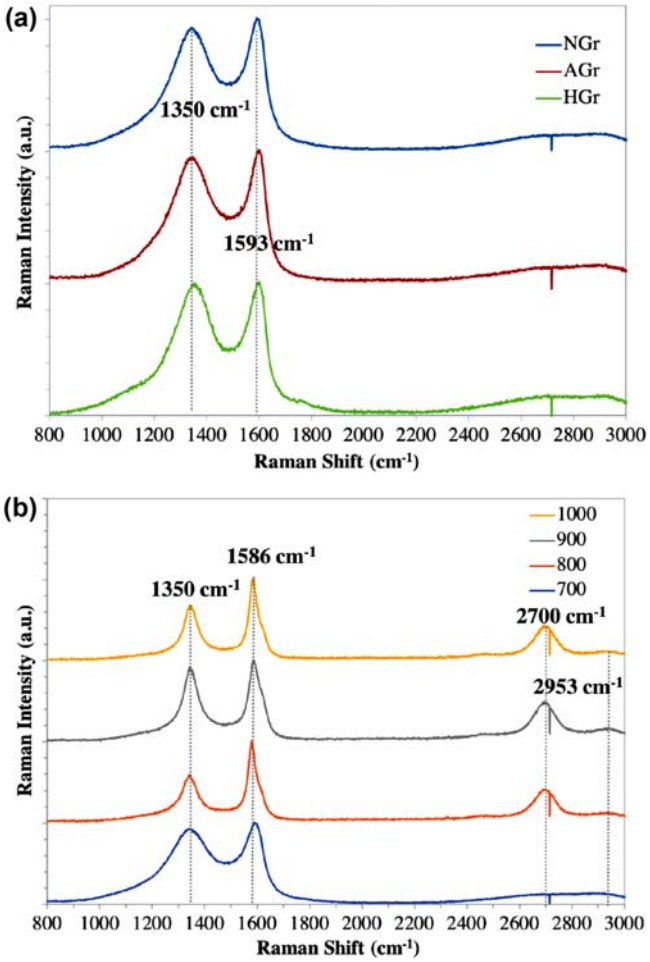

Fig. 4. Raman spectra of (a) gluGr under different inert environments and (b) different carbonization temperature.

gluGr carbonized at 700 °C (NGr700) shows significant differences as compared to other temperatures. NGr700 sample exhibits the highest intensity in D- and G-bands except for 2D-band, which is the lowest among the four samples. From these results, it can be said that the synthesis of graphene from glucose does not completely turn into pure graphene; however, it turns into graphene-like material structure with stacked graphene layers [30]. It is supported with the appearance of high D-band in the spectra, which indicates that the resultant gluGr does not turn into pure graphene, as pure graphene will exhibit almost absent D-band but with sharp G- and 2D-bands. Among all four graphene samples, NGr1000 exhibited the narrowest D, G, and 2D-peaks, which indicates this sample is almost similar to graphene [31]. Moreover, the 2D peak of NGr1000 is the sharpest among the four samples. In NGr700, the 2D peak is shifted to higher frequencies due to the interactions between the graphene layers, and this represents the existence of more graphene layers [7]. Even the NGr700 sample does not become pure graphene; however, this sample possesses the highest SSA as shown in Table 2 (detailed explanation was given previously). In this study, NGr700 is more favorable for gas adsorption due to its high SSA, whereas the gluGr carbonized at higher temperature displayed lower SSA even though they had more graphitic structures. The results show that carbonization conditions and temperatures greatly affect the textural properties of the gluGr samples.

Fig. 5 presents the CH_4 adsorption isotherms of the NGr700 and NGr1000 samples at 25 °C and 35 bar. As expected, adsorption of CH_4 by the gluGr was strongly dependent on their SSA, pore size and pore volume (Table 2). In fact, NGr1000, because of its low SSA (about 239 m^2/g) and small micropore volume (0.328 cm^3/g), showed low CH_4 adsorption capacity of 19.68 cm^3/g, while the CH_4 adsorption of NGr700 sample doubled up the value of NGr1000 due to their larger surface area and higher microporosity. The experimental uptake of CH_4 displays characteristics of Type I adsorption isotherm according to the IUPAC classification. CH_4 uptake drastically increased in the low-pressure region but then steadily increased with further rise of pressure for both samples and reached a maximum at 35 bar. No distinct plateau was observed in the isotherms for the pressure range investigated, indicating that the samples can adsorb greater volume of CH_4 at higher pressure [32]. Combined with the N_2 adsorption tests, the NGr700 sample with narrower pore size distribution (Fig. 4) displays better CH_4 adsorption ability. From the CH_4 adsorption measurements, it is concluded that the CH_4 adsorption on the two gluGr samples

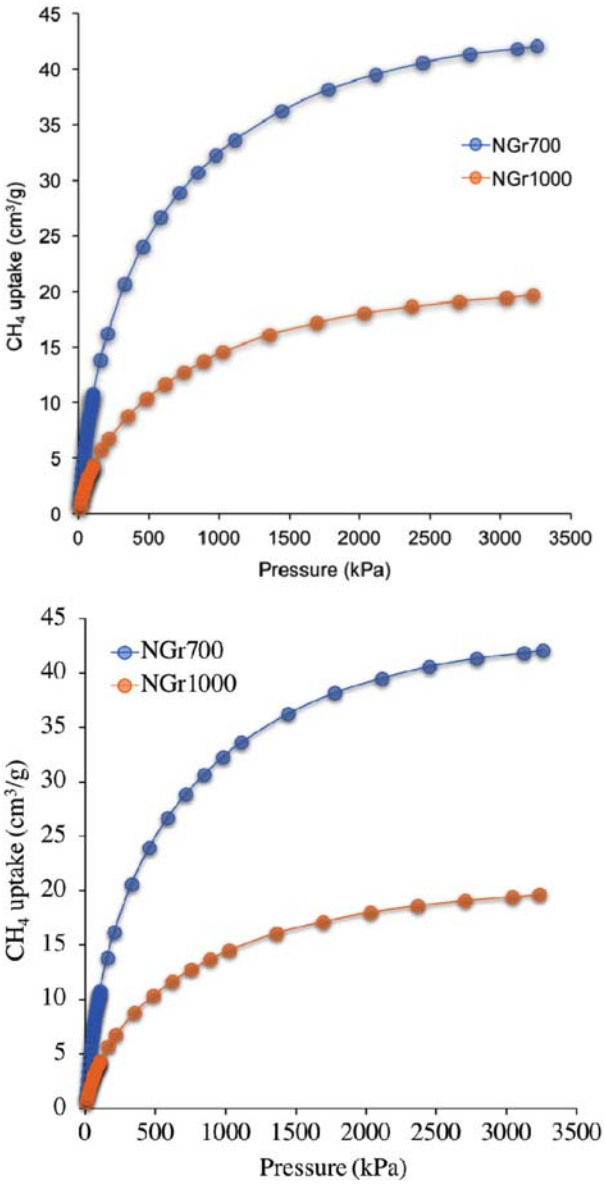

Fig. 5. Methane (CH_4) adsorption isotherms of NGr700 and NGr1000 at 35 bar and 25 °C.

increases along with the micropore volume and the surface area. Accordingly, the NGr700 sample, which had the largest SSA (767 m^2/g), highest pore volume (0.344 cm^3/g), and narrowest pore size distribution ranging between 0.8-1.5 nm, displayed the highest CH_4 uptake of 42.08 cm^3/g at 25 °C and 35 bars.

CONCLUSION

NGr700, with SSA up to 767 m^2/g and total micropore volume of 0.344 cm^3/g, was successfully synthesized through a simple carbonization and $FeCl_3$ activation. The resultant gluGr samples were characterized via Raman spectroscopy, BET method, N_2 adsorption/desorption and were further determined for CH_4 adsorption capacity at 25 °C and 35 bar. A complete CH_4 adsorption uptake was reported with maximum volumetric capacity of up to 42.08 cm^3/g. From the results obtained, it can be obviously seen that the CH_4 adsorption capacity corresponded to the SSA and micropore volumes of all gluGr samples. Due to this, future studies will be focused on improving the SSA (more than 1,000 m^2/g) and microporosity of the samples in order to attain even higher adsorption capacity of CH_4.

ACKNOWLEDGEMENTS

The authors would like to acknowledge the financial support from the Malaysian Ministry Education and Universiti Teknologi Malaysia under UTM-TDR grant scheme (Q.J130000.3551.06G07), CRG grant (Q.J130000.2451.08G26), Malaysia Research University Network Grant Scheme (MRUN) (R.J130000.7851.4L865), UTM award grant (R.J130000.7351.5M002), and UTM Prototype Research grant (Q.J130000.2851.00L41). One of the authors, F.E.C. Othman, would like to acknowledge the Zamalah Scholarship received from UTM and NIMS Internship Scholarship 2018 awarded by National Institute of Materials Science (NIMS), Japan. The authors would also like to acknowledge the technical and management support from Research Management Centre (RMC), Universiti Teknologi Malaysia.

CONFLICT OF INTEREST

There is no potential conflict of interest reported by the author(s).

REFERENCES

1. K. S. Novoselov, A. K. Geim, S. V. Morozov, D. Jiang, Y. Zhang, S. V. Dubonos, I. V. Grigorieva and A. A. Firsov, *Science*, **306**, 666 (2004).
2. M. Sang, J. Shin, K. Kim and K. J. Yu, *Nanomaterials*, **9**, 374 (2019).
3. A. Hassani, M. T. H. Mosavian, A. Ahmadpour and N. Farhadian, *Korean J. Chem. Eng.*, **34**, 876 (2017).
4. S. Chowdhury and R. Balasubramaniam, *Ind. Eng. Chem. Res.*, **55**, 7906 (2016).
5. S. A. Bhuyan, N. Uddin, M. Islam and F. A. Bipasha, *Int. Nano Lett.*, **6**, 63 (2016).
6. S. Gadipelli and Z. X. Guo, *Prog. Mater. Sci.*, **69**, 1 (2015).
7. T. Purkait, G. Singh, M. Singh, D. Kumar and R. S. Dey, *Sci. Rep.*, **7**, 1 (2017).
8. J. M. Berg, J. L. Tymoczko and L. Stryer, *Biochemistry 5th Ed.* W. H. Freeman and Company, New York (2002).
9. T. Hongo, J. Sugiyama, A. Yamazaki and A. Yamasaki, *Ind. Eng. Chem. Res.*, **52**, 2111 (2013).
10. Y. Chen, X. Zhang, H. Zhang, X. Sun, D. Zhang and Y. Ma, *RSC Adv.*, **2**, 7727 (2012).
11. D. Prahas, Y. Kartika, N. Indraswati and S. Ismadji, *Chem. Eng. J.*, **140**, 32 (2008).
12. W. Tongpoothorn, M. Sriuttha, P. Homchan, S. Chanthai and C. Ruangviriyachai, *Chem. Eng. Res. Des.*, **89**, 335 (2011).
13. Z. Jiang, Y. Liu, X. Sun, F. Tian, F. Sun, C. Liang, W. You, C. Han and C. Li, *Langmuir*, **19**, 731 (2003).
14. D. P. Vargas, L. Giraldo and J. C. Moreno-Pirajan, *Adsorption*, **22**,

717 (2016).
15. T. E. Rufford, D. Hullicova-Jurcakova, Z. Zhu and G. Q. Lu, *J. Mater. Res.*, **25**, 1451 (2011).
16. J. Sahira, A. Mandira, P. B. Prasad and P. R. Ram, *Res. J. Chem. Sci.*, **3**, 19 (2013).
17. Z. Xu, Z. Yuan, D. Zhang, W. Chen, Y. Huang, T. Zhang, D. Tian, H. Deng, Y. Zhou and Z. Sun, *J. Cleaner Prod.*, **192**, 453 (2018).
18. P. Singh, J. Bahadur and K. Pal, *Graphene*, **6**, 61 (2017).
19. X. H. Li, S. Kurasch, U. Kaiser and M. Antonietti, *Angew. Chem. Int. Ed.*, **51**, 9689 (2012).
20. M. Danish, R. Hashim, M. N. M. Ibrahim and O. Sulaiman, *J. Anal. Appl. Pyrol.*, **104**, 418 (2013).
21. B. Zhang, J. Song, G. Yang and B. Han, *Chem. Sci.*, **5**, 4656 (2014).
22. J. Jagiello and M. Thommes, *Carbon*, **42**, 1227 (2004).
23. N. Indayaningsih, F. Destyorini, R. I. Purawiardi, D. R. Insiyanda and H. Widodo, *IOP Conf. Ser.: J. Phys. Conf. Ser.*, **817**, 1 (2016).
24. C. Song, T. Wang, J. S. Qiu, Y. M. Cao and T. Cai, *J. Porous Mater.*, **15**, 1 (2008).
25. E. J. Amieva, J. Lopez-Barroso, A. L. Martinez-Hernandez and C. Velasco-Santos, *Graphene-based materials functionalization with natural polymeric biomolecules*, INTECH Open Access, United Kingdom (2016).
26. J. C. Groen, L. A. A. Peffer and J. Perez-Ramirez, *Micropor. Mesopor. Mater.*, **60**, 1 (2003).
27. S. Wang, Q. Feng, M. Zha, F. Javadpour and Q. Hu, *Energy Fuel*, **32**, 169 (2018).
28. A. Kaniyoor and S. Ramaprabhu, *AIP Adv.*, **2**, 1 (2012).
29. E. I. Biru and H. Iovu, *Graphene nanocomposites studied by Raman spectroscopy*, INTECH Open Access, United Kingdom (2018).
30. J. B. Wu, M. L. Lin, X. Cong, H. N. Liu and P. H. Tan, *Chem. Soc. Rev.*, **47**, 1822 (2018).
31. Q. A. Khan, A. Shaur, T. A. Khan, Y. F. Joya and M. S. Awan, *Cogent Chem.*, **3**, 1 (2017).
32. S. Himeno, T. Komatsu and S. Fujita, *J. Chem. Eng. Data*, **50**, 369 (2005).